

Biosynthesis of Silver Nanoparticles Mediated by *Lippia graveolens* Aqueous Extract

Karen M. Soto¹, Montserrat Hernández-Iturriaga², Arely Cárdenas³, Sandra Mendoza^{2*}

¹Centro de Investigaciones y de Estudios Avanzados del I.P.N. Unidad Querétaro, Querétaro, Querétaro, C.P. 76230, Mexico.

²Departamento de Investigación y Posgrado en Alimentos, Facultad de Química, Universidad Autónoma de Querétaro. Querétaro, Qro 76010, México.

³Consejo Nacional De Ciencia y Tecnología (CONACYT)- Centro de Investigación en Química para la Economía Circular, CIQEC, Facultad de Química, Universidad Autónoma de Querétaro. Querétaro, Qro 76010, México.

*Corresponding author: Sandra Mendoza, email: smendoza@uaq.mx

Received May 27th, 2023; Accepted October 10th, 2023.

DOI: <http://dx.doi.org/10.29356/jmcs.v68i3.2070>

Abstract. The synthesis of silver nanoparticles (AgNPs) with plant extracts has acquired a lot of interest in recent years, due to its different applications in areas such as medicine, optics, food, pharmaceutical, among others. The aim of this work was to evaluate aqueous extracts of Mexican oregano (*Lippia graveolens*), rich in antioxidant compounds, to synthesize AgNPs. *L. graveolens* extract was characterized by HPLC and the antioxidant capacity was evaluated by ABTS, DPPH and CUPRAC. The effect of factors such as pH, concentration of precursor and temperature on the synthesis of AgNPs was studied. The particles were characterized by SEM, TEM, FTIR and their stability was evaluated with respect to time. The AgNPs showed a spherical shape with an average diameter of 2.4 nm, and antimicrobial activity against *S. aureus*, *L. monocytogenes* and *E. coli*. After 30 days of storage, the AgNPs agglomerated to form dendritic structures.

Keywords: Silver nanoparticles; Mexican oregano; antimicrobial activity; green synthesis.

Resumen. La síntesis de nanopartículas de plata (AgNPs) mediante extractos de plantas ha adquirido interés en años recientes debido a los diversos campos donde pueden usarse, como la medicina, óptica, alimentos, farmacéutica, entre otras. El objetivo de esta investigación fue evaluar la capacidad de extractos acuosos del orégano mexicano (*Lippia graveolens*), rico en compuestos antioxidantes, para sintetizar AgNPs. El extracto de *L. graveolens* fue caracterizado por HPLC y la actividad antioxidante fue evaluada mediante los ensayos de ABTS, DPPH y CUPRAC. Se estudió el efecto del pH, concentraciones de precursor, y temperatura en la síntesis de AgNPs. Las partículas fueron caracterizadas mediante SEM, TEM, FTIR y su estabilidad con respecto al tiempo fue evaluada. Las AgNPs presentaron una forma esférica con diámetro promedio de 2.4 nm, y actividad antimicrobiana contra *S. aureus*, *L. monocytogenes* and *E. coli*. Después de 30 días de almacenaje, las AgNPs se aglomeraron formando estructuras dendríticas.

Palabras clave: Nanopartículas de plata; orégano mexicano; actividad antimicrobiana; síntesis verde.

Introduction

Metallic nanoparticles in a nano size scale show unique characteristics with extensive applications in diverse fields such as agriculture, cosmetics, pharmaceuticals, medicine, textiles, and food industry [1]. Silver is the metal of first choice to produce nanoparticles due to its high antimicrobial activity against a wide range of bacteria and fungi as well as its catalytic properties [2,3]. Physical and chemical methods have been used to synthesize NPs but they are environmentally hazardous, technically laborious, and expensive [4]. To overcome these limitations, green synthesis methods have been proposed to obtain silver and gold nanoparticles (AgNPs, AuNPs) where antioxidants, plant extracts and microorganisms are used as reductant reagents [5]. The use of plant extracts has the advantages of being scalable and less expensive than the methods based on microbial processes; on the other hand, the rate of reduction of metal ions using plants has been found to be much faster as compared to microorganisms affording stable metal nanoparticles [6,7]. Several reviews highlight the synthesis, characterization, and application of plant-based metallic nanoparticles [8-10]. The secondary metabolites of plants (terpenoids, phenolic acids and flavonoids) act as reducing and stabilizing agents in the synthesis of metal nanoparticles, then the source of the plant extract and the extraction process influence the characteristics of the NPs [11,12].

Most of the aromatic oregano plants belong to the genus *Origanum* (Lamiaceae) and *Lippia* (Verbenaceae). Among the aromatic plants used to produce AgNPs, *Origanum vulgare* better known as European oregano, has been reported to generate spherical AgNPs sizes of 136 nm [13] and 1 to 50 nm [14]. *Lippia graveolens* KHB, commonly known as Mexican oregano, is used as condiment of many traditional Mexican dishes as well as raw material to produce cosmetics, drugs, and liquors. In Latin America, *L. graveolens* is used as antiseptic, antipyretic, analgesic, antispasmodic, antioxidant and antimicrobial agent [15]. The aqueous extract of *L. graveolens* has many secondary metabolites being the most abundant flavonoids and terpenoids which are responsible of the observed antioxidant activity [16-18]. The reducing power of *L. graveolens* extracts can mediate the synthesis of metallic nanoparticles. In the present study, AgNPs were obtained by an aqueous extract of *Lippia graveolens*, the effect of extract concentration, reaction time, temperature and pH of the reaction medium was analyzed. The obtained nanoparticles were physicochemical characterized, and the antimicrobial activity was tested against food pathogens.

Methodology

Materials

2,2'-azinobis-3-ethylbenzothiazoline-6-sulfonic acid (ABTS), potassium persulfate, Trolox, 1,1-diphenyl-2-picrylhydrazyl (DPPH), Folin & Ciocalteu's reagent and HPLC standards were obtained from Sigma Chemical Co. (St. Louis MO, U.S.A.). Agar (TSA), and Tryptic soy broth (TSB) were purchased from Becton-Dickinson (New Jersey, USA). All solvents, and silver nitrate were obtained from Baker (Mallinckrodt Baker, Inc., Phillipsburg, NJ, USA). Ammonium acetate, copper (II) chloride, sodium hydroxide, sodium carbonate, copper (II) sulfate, potassium persulfate, methanol, sodium potassium tartrate and 96% EtOH were obtained from Merck (Darmstadt, Germany).

Lippia graveolens extract preparation and characterization

10 g of the dried plant were taken and mixed with 100 mL of deionized water and heated at 60 °C for 10 min. After cooling at room temperature, the mixture was filtered with a Whatman No.1 filter paper and the aqueous filtrate was lyophilized and stored for future use. The antioxidant activity of the extract was evaluated by the DPPH, ABTS and electrochemical CUPRAC (cupric ion reducing antioxidant capacity) assays according to reported procedures [19-21] and the results were expressed as IC₅₀ in mg/L. The total phenolic content of the extract was determined by Folin-Ciocalteu colorimetric method [22] expressing the results as mg of gallic acid equivalents per g dried sample (mg GA/g dw). The HPLC-DAD method reported by Ramírez-Jiménez *et al.* [23] was used to obtain the phenolic profile of the extract. The external standard method was used to quantify

the secondary metabolites in an Agilent 2100 Series HPLC system (Agilent Technologies, Palo Alto, CA, USA) using a Sorbax Eclipse XDB-C18 column (Agilent Technologies, 9.4 x 250 mm, 5.0 μ m).

Biosynthesis of silver nanoparticles

To study the effect of pH (2, 5, 8, 10), temperature (20, 60, 80 °C) and reaction time (5, 10, 15, 20 min) on the AgNPs formation, solutions containing 20 mg of lyophilized oregano aqueous extract and AgNO₃ 1mM were used. Values of pH were adjusted by using 0.1 N NaOH and 0.1 N HCl after the addition of the extract. The temperature used for pH experiments was 20 °C and for reaction time 80 °C. The AgNPs formation was monitored by UV-Vis spectrophotometry (200-800 nm) (Spectra Max Tunable Microplate Reader, Molecular Devices Co., Sunnyvale, CA, USA). The colloidal suspensions were centrifuged at 15,000 rpm, washed three times with distilled water and dried at 60 °C, the powder was kept for further characterization.

Silver nanoparticle characterization

Infrared absorption spectra of dried AgNPs and dried extracts were recorded by DRIFT with 4 cm⁻¹ of resolution (Spectrum GX spectrophotometer, Perkin Elmer, Massachusetts, USA with a diffuse reflectance accessory, Pike Technology model). The morphology and size of AgNPs were obtained from a JEOL (Japan) high-resolution transmission electron microscope (JEM-1010) and a Carl Zeiss (Jena, Germany) high-resolution scanning electron microscope (EVO-50). Image J software was used to calculate the diameters of the NPs (average of 50 NPs).

Stability of silver nanoparticles

The colloidal solutions obtained after biosynthesis of silver nanoparticles (pH 5, 80 °C, 5 min), were stored at room temperature for 30 days. Every five days UV-Visible spectra was recorded, and at the end of the experiment the AgNPs solution was characterized by TEM.

Antimicrobial activity

To evaluate the antimicrobial activity of the AgNPs, the agar well diffusion technique was used against *Escherichia coli* (ATCC 25922), *Listeria monocytogenes* (ATCC 35152) and *Staphylococcus aureus* (ATCC 6538). The methodology described by Soto et al. [24] was followed. Briefly, five μ L (10⁵ CFU/mL) of each microorganism culture were suspended in 6 mL of ST agar tempered at 45 °C, mixed and immediately poured into a Petri dish. Once agar solidified, 10 μ L of AgNPs solution (20, 40, 60, 70, 80, 90 and 100 μ g/mL) were placed on the agar surface, then incubated for 48 h at 30 °C and the zone of growth inhibition was measured. Oregano lyophilized extract (100 μ g/mL) and chloramphenicol (500 μ g/mL) were used as control.

Results and discussion

Characterization of Lippia graveolens extract

Table 1 shows the identified compounds by HPLC-DAD of lyophilized *L. graveolens* extract. Rosmarinic, gallic and ellagic acids, kaempferol and thymol were the major components among the identified secondary metabolites, this result is similar to the reported data by Herrera-Rodríguez *et al.* [25] who evaluated the phenolic compounds in the essential oil of *L. graveolens* by GC/MS analysis. Thymol was detected in a higher concentration than Greek oregano (10.6 μ g/g) under similar extraction conditions [26]. The antioxidant activity of the aqueous extract was evaluated by ABTS, DPPH and CUPRAC techniques, the first two methods are based on electron transfer from the secondary metabolites of the extracts to the radicals while the last one evaluates the electron-donating capacity of the extract to reduce a metal complex [27]. IC₅₀ values of 229.4 \pm 10.5 mg/L, 290.1 \pm 12.7 mg/L, and 95.01 \pm 0.69 mg/L for ABTS, DPPH and CUPRAC assays were obtained, respectively. The antioxidant activity of the extract was similar to the reported values (IC₅₀ 207 mg/L) for methanolic extracts from *L. graveolens* evaluated by the DPPH assay [15]. As expected, the antioxidant values were lower than the aqueous extracts from *O. vulgare* (26.7 mg/L) [28]. The total phenol content was 330.5 \pm 1.7 mg GAE/g dw, this value is higher than the reported values for several hydroethanolic extracts from *L.*

graveolens samples (95.74- 99.71mg GAE/g dw) [29]. Rosmarinic acid, thymol and kaempferol are the secondary metabolites that significantly contribute to the antioxidant capacity of the extract.

Table 1. Phenolic compounds in *Lippia graveolens* determined by HPLC-DAD

Retention time (min)	Compound	Concentration mg/g dw	% Adjust
<i>Phenolic acids</i>			
3.22	Gallic acid	1.31 ± 0.39	93.9
3.97	Protocatechuic acid	0.26 ± 0.02	97.9
5.44	Ellagic acid	1.86 ± 0.05	94.6
5.65	Coumaric acid	0.96 ± 0.07	96.5
5.76	Rosmarinic acid	2.46 ± 0.19	99
5.9	Ferulic acid	0.62 ± 0.03	99.8
<i>Aldehyde</i>			
6.16	Vanillin	0.87 ± 0.01	97.9
<i>Flavonoids</i>			
7.44	Quercetin	0.81 ± 0.09	99.7
14.69	Apigenin	0.63 ± 0.04	98.7
14.91	Kaempferol	5.76 ± 0.03	92.3
4.68	Naringenin	0.48 ± 0.05	98.3
<i>Monoterpene</i>			
15.22	Thymol	3.12 ± 0.06	93.7

Results reported as mean ± standard error of three replicates. The concentration is reported as mg/g of dried sample.

Biosynthesis of silver nanoparticles in different conditions

The green synthesis of AgNPs with plant extracts is mediated by the compounds that have enough electrochemical potential to reduce silver ions, then the chemical state and concentration of the extract components affect the size and shape of the nanoparticles [30]. It has been demonstrated by several authors that green synthesis of AgNPs involves the reduction of Ag^+ to Ag^0 by antioxidant secondary metabolites, in this case mainly rosmarinic acid, thymol and kaempferol. Then nucleation and growth of Ag^0 nanoparticles occur to finally be covered by the oxidized secondary metabolites, this final stage favours the stabilization of the NPs [8-10,24].

Here, colloidal solutions of AgNPs were prepared by adding different concentrations of AgNO_3 to an aqueous solution of the oregano extract, the solutions changed their colour from transparent to dark yellow within minutes, indicating the presence of AgNPs. The effect of silver nitrate concentration is shown in Fig. 1(a), the characteristic AgNPs surface plasmon resonance (SPR) absorption band was observed at 357-400 nm. The band absorption increased, and the wavelength was shifted to the red as AgNO_3 concentration increased from 1 mM to 4 mM. Similar results were reported for the obtention of AgNPs from an aqueous extract of *Oscillatoria limnetica*, addition of the silver nitrate concentration from 0.1 mM to 0.5 mM shifted the surface plasmon bands from 422 nm to 430 nm with gradual intensity increase (0.531-0.710) [31].

Considering the SPR response, further experiments were conducted using 1 mM AgNO₃. Fig. 1(b) shows the absorption spectra of colloidal solutions at different temperatures (20-80 °C). With the increase of temperature, the reduction of silver salt is enhanced, as indicated by the rapid color change of the solution. The peak absorption wavelength shifted toward blue from 437 to 400 nm with the temperature increment. As reported, this displacement indicates that the size of the synthesized nanoparticles decreases with increasing temperature, which may be due to a faster reaction rate at higher temperature. It is generally accepted that high temperature promotes Ag nucleation while low temperature allows the growth of AgNPs, then smaller particles with uniform size distribution are formed at higher temperature [32,33].

The pH plays an important role in the nanoparticle's synthesis because the electron transfer from the secondary metabolites to the silver ions depends on the molecular ionization, also the charge of biomolecules might affect AgNPs capping as well as stabilizing properties [34]. Fig. 1(c) shows the spectra of AgNPs synthesized under different pH values at 80 °C, this temperature was chosen considering that smaller AgNPs were obtained. At pH 2 two absorption bands at 365 and 443 nm were observed. It has been reported that the AgNPs with nanocube morphology exhibit two dipole plasmonic peaks, one belongs to oscillating charges along longitudinal axis, and the other one belongs to oscillating charges along latitudinal axis [35]. For pH 5, 8 and 10 only one band was observed at 400, 375 and 442 nm, respectively. In basic pH values the synthesis of silver nanoparticles is faster than at acid pH, the change of color was observed immediately, but when the solution was heated precipitation was observed. Verma and Mehata [34] observed that at high pH values the particles became unstable and agglomerated, when kept overnight. For this study, AgNPs synthesis at pH 5 shows the major absorbance and the more defined band at lower wavelength which is related to small nanoparticles and homogeneous distribution of the particle size [36]. In other studies, it was reported that basic pH promotes the synthesis of silver nanoparticles due to deprotonation of organic acids such as citric and malic acid [37].

The effect of time reaction was evaluated using AgNO₃ 1mM, pH 5 and 80 °C. Fig. 1(d) shows the spectra of AgNPs at different reaction times, after ten minutes of reaction no SPR wavelength displacements were observed. The increment of the SPR absorption band indicates an enhancement in the formation of AgNPs. The reaction was completed at 30 min and a precipitate was obtained.

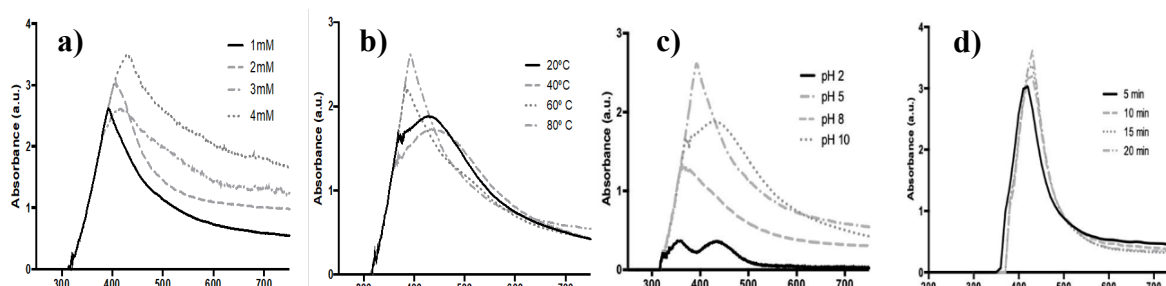


Fig. 1. UV-Visible spectra of synthesized AgNPs using aqueous extract of *L. graveolens* at different parameters. (a) AgNO₃ concentration, (b) 1 mM AgNO₃ at different temperatures, (c) 1 mM AgNO₃ at different pH and (d) 1 mM AgNO₃ at different reaction time.

Characterization of AgNPs

The synthesis of AgNPs was conducted in the optimal conditions established in the previous experiment (AgNO₃ 1mM, pH 5, 80 °C and 10 min). Fig. 2 shows the morphology of nanoparticles obtained by SEM and TEM, the AgNPs were spherical with diameters between 1-4 nm. Several plant extracts have been used to synthesize spherical AgNPs with sizes ranging from 0.5 nm to 100 nm [8-10]. The oregano AgNPs obtained here are smaller than those obtained from European oregano (*Origanum vulgare*) aqueous extract (136 nm) [18], and ethanolic extract (30-58 nm) [19]. Similar size was reported for AgNPs obtained from *Polygonatum graminifolium* (3-15 nm) [38], *Coriandrum sativum* (6.95 nm) [39], *Sida cardifolia* (3-8 nm) [40], *Piper retrofractum* (1-5 nm) [41], and *Allium sativum* (3-6 nm) [42].

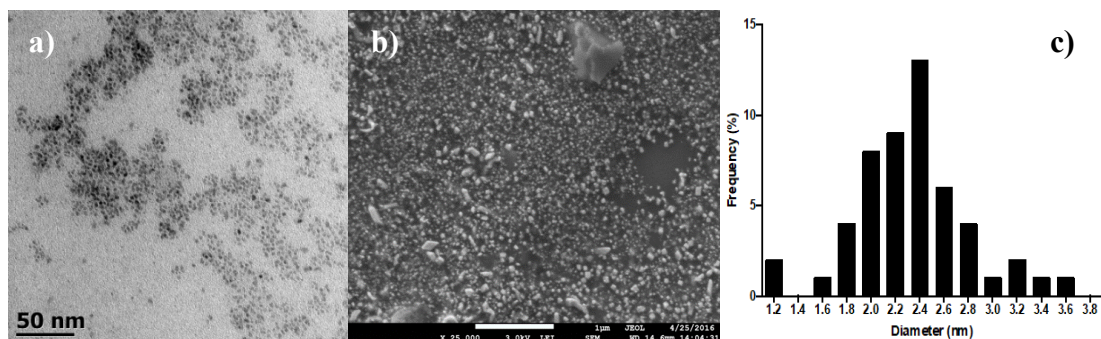


Fig. 2. (a) TEM and (b) SEM images of AgNPs and (c) size distribution.

Fig. 3 shows the DRIFT spectra for the dried extract, where the typical fingerprint region from 800 to 1800 cm^{-1} attributed to the stretching and bending vibrations characteristic of the *L. graveolens* secondary metabolites is observed [43]. This region included the signals at 1100-1400 cm^{-1} corresponding to C-O of hydroxyl groups, bands at 1400-1500 cm^{-1} corresponding to C-O and C-C stretching vibrations specific to phenyl groups, signals at 1500-1600 cm^{-1} corresponding to aromatic domain and N-H bending, and the region at 1600-1800 cm^{-1} corresponding to bending N-H, C=O stretching's signals assigned to aldehydes, ketones, and esters [43,44]. Other important band observed was at 3000-3700 cm^{-1} corresponding to O-H stretching vibrations. The spectra of the dried AgNPs displayed most of the DRIFT bands of the extract, which confirm that the secondary metabolites play the role of capping and stabilizing agents in the synthesis of AgNPs. Some displacements were observed for some bands that represent the interactions of functional groups with AgNPs surface [45].

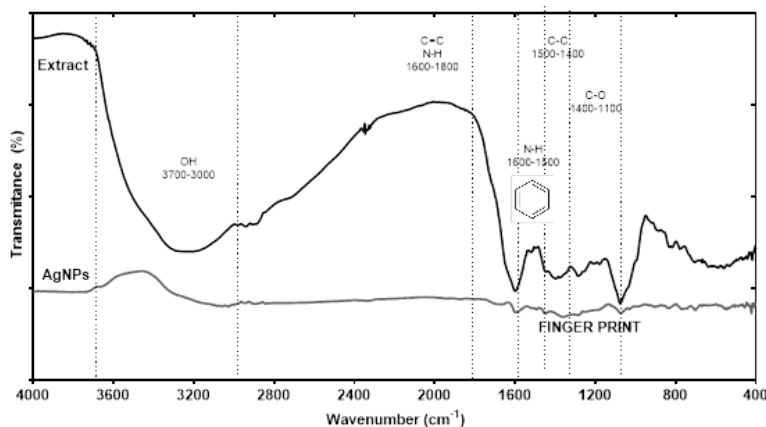


Fig. 3. DRIFT of lyophilized *L. graveolens* extract and dried AgNps.

Stability of AgNPs

Fig. 4(a) shows the UV-Vis spectra of AgNPs at different times of storage. After fifteen days of storage at room temperature, the AgNPs SPR signal changed drastically, and after a month under storage, the colour of the AgNPs solution turned dark- gray and a sediment was formed. As storage time increase, the SPR signal gets wider and shifted to higher wave numbers, confirming changes of shape and size of the nanoparticles. After one month of storage, the SEM and TEM images (Fig. 4(b)-(c)) evidenced AgNPs clustering with a morphology which has been denominated flower-like [46]. It has been proposed that the formation of the dendritic structures involves the aggregation of NPs to form micrometric worm-like structures that serve as template for the growth of multi-branched structures [47]. These dendritic structures can be used in catalysis, and antimicrobial metallic coatings, among other applications [48,49].

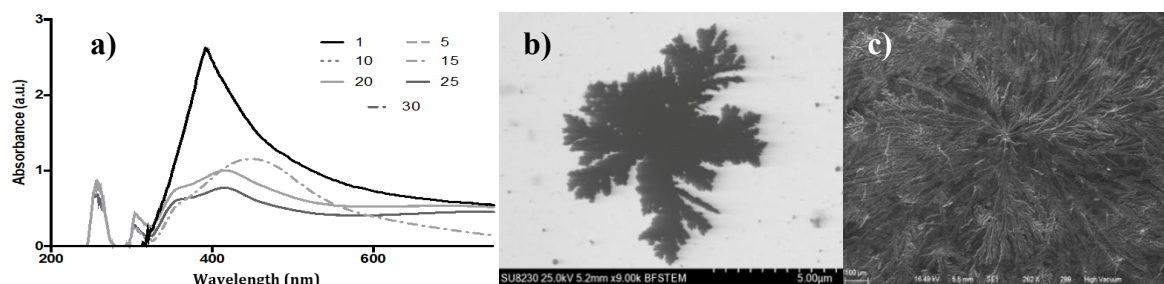


Fig. 4. (a) UV-Vis spectra of AgNPs at different days of storage. (b) TEM image after 30 days of storage, and (c) SEM image after 30 days of storage.

Antimicrobial activity

Table 2 shows the diameter of growth inhibition zones produced by oregano extract and AgNPs against three food pathogens, *S. aureus*, *L. monocytogenes* and *E. coli*. For all tested microorganism, the AgNPs antimicrobial activity was concentration dependent, and the results revealed that the AgNPs displayed significant inhibition activity against all the tested pathogens. Although, *L. monocytogenes* and *S. aureus* are Gram positive with a thicker membrane cell compared to Gram negative microorganism such as *E. coli*, both demonstrated sensitivity to the antimicrobial effect of AgNPs. Similar results were reported by Ruíz-Baltazar et al. [50] where AgNPs synthesized with *Melissa officinalis* leaf extract, at 15 and 20 mM exhibited growth inhibition diameters of 12.5 and 11.5 mm against *S. aureus* and *E. coli*, respectively. Sankar et al. [13] evaluated the antimicrobial activity of AgNPs (30 µL) obtained from *O. vulgare* extract against *E. coli* obtaining a 10 mm growth inhibition diameter. Several factors are to be considered regarding AgNPs antimicrobial activity, the electronic effect produced by the interaction of silver with bacterial membrane surface, the chemical structure of secondary metabolites that stabilized the AgNPs when synthesized by plant extracts, and the shape and size of NPs [7,51]. All the evaluated AgNPs concentrations showed higher antimicrobial activity compared with *L. graveolens* extract [52,53]. The antimicrobial activity of the Mexican oregano has been mainly attributed to the terpenes like thymol and eugenol as well as phenolic acids like rosmarinic acid (15,29,52). As expected, the antimicrobial activity of the AgNPs were higher than the extract, since the antimicrobial activity produce by the release of Ag⁺ ions is added to the antimicrobial activity of the secondary metabolites that surrounded the NPs (8-10). At the maximum AgNPs concentration (100 µg/mL), the antimicrobial effect against *E. coli* and *S. aureus* was higher than chloramphenicol.

Table 2. Diameter of growth inhibition zone of AgNPs against *S. aureus*, *E. coli* and *L. monocytogenes*.

Concentration (µg/mL)	<i>S. aureus</i> Diameter (mm)	<i>L. monocytogenes</i> Diameter (mm)	<i>E. coli</i> Diameter (mm)
20	9.36 ± 0.15 ^c	8.52 ± 0.06 ^f	9.46 ± 0.11 ^f
40	10.16 ± 0.19 ^{dc}	9.64 ± 0.12 ^c	10.27 ± 0.09 ^c
60	11.06 ± 0.11 ^d	10.89 ± 0.04 ^d	10.71 ± 0.07 ^{dc}
70	12.60 ± 0.16 ^c	11.15 ± 0.09 ^d	11.63 ± 0.11 ^c
80	13.53 ± 0.17 ^{bc}	11.59 ± 0.05 ^c	13.38 ± 0.03 ^b
100	14.87 ± 0.45 ^a	12.58 ± 0.10 ^b	13.95 ± 0.06 ^a
Extract (100 µg/mL)	7.56 ± 0.14 ^f	7.90 ± 0.05 ^g	7.5 ± 0.11
Chloramphenicol (500 µg/mL)	13.95 ± 0.39 ^{ab}	14.80 ± 0.05 ^a	10.80 ± 0.08 ^d

Results reported as mean ± standard error of three replicates. Different letters in the same column represent significance difference (P<0.05) according to the Tukey test n=3.

Conclusions

Silver nanoparticles have been successfully synthesized using *L. graveolens* extract, the AgNPs are spherical and exhibit a high energy SPR band around 400 nm. According to the FTIR analysis, the compounds present in *L. graveolens* extract play an important role in the reduction and stabilization of metal nanoparticles. The obtained AgNPs are stable in colloidal solution for 15 days, after which the nanoparticles agglomerated and formed dendritic structures, meaning that the use of oregano AgNPs on liquid products that need to be stored for more than 15 days is not recommended. The AgNPs antimicrobial activity is dependent on the concentration and has better activity against *S. aureus* and *E. coli*. The obtained AgNPs can be used in different applications due to its biological activity and morphology.

References

1. Ahmad, S.; Munir, S.; Zeb, N.; Ullah, A.; Khan, B.; Ali, J.; Bilal, M.; Omer, M.; Alamzeb, M.; Salman, S. M.; Ali, S. *Int. J. Nanomedicine*. **2019**, *14*, 5087–5107. DOI: <https://doi.org/10.2147/IJN.S200254>.
2. Saha, J.; Begum, A.; Mukherjee, A.; Kumar, S. *Sustain. Environ. Res.* **2017**, *27*, 245–250. DOI: <https://doi.org/10.1016/j.serj.2017.04.003>.
3. Sharma, V.; Kaushik, S.; Pandit, P.; Dhull, D.; Yadav, J. P.; Kaushik, S. *Appl. Microbiol. Biotechnol.* **2019**, *103*, 881–891. DOI: <https://doi.org/10.1007/s00253-018-9488-1>.
4. Pattanayak, S.; Rahaman, M.; Maity, D.; Chakraborty, S.; Kumar, S.; Chattopadhyay, S. *J. Saudi Chem. Soc.* **2017**, *21*, 673–684. DOI: <https://doi.org/10.1016/j.jscs.2015.11.004>.
5. Sudha, A.; Jeyakanthan, J.; Srinivasan, P. *Resource-Efficient Technologies*. **2017**, *3*, 506–515. DOI: <https://doi.org/10.1016/j.reffit.2017.07.002>.
6. Castillo-Henríquez, L.; Alfaro-Aguilar, K.; Ugalde-álvarez, J.; Vega-Fernández, L.; de Oca-Vásquez, G. M.; Vega-Baudrit, J. R. *Nanomater.* **2020**, *10*, 1–24.
7. Kumar, A.; Chisti, Y.; Chand, U. *Biotechnol. Adv.* **2013**, *31*, 346–356. DOI: <https://doi.org/10.1016/j.biotechadv.2013.01.003>.
8. Alshameri, A.W.; Owais, M. *OpenNano*. **2022**, *8*, 100077. DOI: <https://doi.org/10.1016/j.onano.2022.100077>.
9. Hasan, K. M.; Xiaoyi, L.; Shaoqin, Z.; Horváth, P. G.; Bak, M.; Bejó, L.; Sipos, G.; Alpár, T. *Heliyon*. **2022**, *8*, e12322. DOI: <https://doi.org/10.1016/j.heliyon.2022.e12322>.
10. Nadaf, S.J.; Jadhav, N. R.; Naikwadi, H. S.; Savekar, P. L.; Sapkal, I.D.; Kambli, M.M.; Desai, I. A. *OpenNano*. **2022**, *8*, 100076. DOI: <https://doi.org/10.1016/j.onano.2022.100076>.
11. Gopinath, K.; Venkatesh, K. S.; Ilangovan, R.; Sankaranarayanan, K.; Arumugam, A. *Ind. Crops Produ.* **2013**, *50*, 737–742. DOI: <https://doi.org/10.1016/j.indcrop.2013.08.060>.
12. Sulaiman, G. M.; Mohammed, W. H.; Marzoog, T. R.; Al-, A. A. A.; Kadhum, A. A. H.; Mohamad, A. B. *Asian Pac. J. Trop. Biomed.* **2013**, *3*, 58–63. DOI: [https://doi.org/10.1016/S2221-1691\(13\)60024-6](https://doi.org/10.1016/S2221-1691(13)60024-6).
13. Sankar, R.; Karthik, A.; Prabu, A.; Karthik, S.; Subramanian, K.; Ravikumar, V. *Colloids Surf. B: Biointerfaces*, **2013**, *108*, 80–84. DOI: <https://doi.org/10.1016/j.colsurfb.2013.02.033>.
14. Hambardzumyan, S.; Sahakyan, N.; Petrosyan, M.; Nasim, M. J.; Jacob, C.; Trchounian, A. *AMB Express*. **2020**, *10*. DOI: <https://doi.org/10.1186/s13568-020-01100-9>.
15. Martínez-Rocha, A.; Puga, R.; Hernández-Sandoval, L.; Loarca-Piña, G.; Mendoza, S. *Plant Foods Hum. Nutr.* **2008**, *63*, 1–5 DOI: <https://doi.org/10.1007/s11130-007-0061-9>.
16. González-Fuentes, F.; López-Gil, M.A.; Mendoza S.; Escarpa A. *Electroanalysis*. **2011**, *9*, 2212–2216. DOI: <https://doi.org/10.1002/elan.201100245>.
17. Cortés-Chitala, M. D. C.; Flores-Martínez, H.; Orozco-Ávila, I.; León-Campos, C.; Suárez-Jacobo, Á.; Estarrón-Espinosa, M.; López-Muraira, I. *Molecules*. **2021**, *26*. DOI: <https://doi.org/10.3390/molecules26030702>.

18. Soto-Domínguez, A.; García-Garza, R.; Ramírez-Casas, Y.; Morán-Martínez, J.; Serrano-Gallardo, L. B. *Int. J. Morphol.* **2012**, *30*, 937–944. DOI: <https://doi.org/10.4067/S0717-95022012000300029>.
19. Cárdenas, A.; Gómez, M.; Frontana, C. *Electrochim. Acta.* **2014**, *128*, 113–118. DOI: <https://doi.org/10.1016/j.electacta.2013.10.191>.
20. Fukumoto, L. R.; Mazza, G. J. *J. Agric. Food Chem.* **2000**, *48*, 3597–3604. DOI: <https://doi.org/10.1021/jf000220w>.
21. Nenadis, N.; Wang, L. F.; Tsimidou, M.; Zhang, H. Y. *J. Agric. Food Chem.* **2004**, *52*, 4669–4674. DOI: <https://doi.org/10.1021/jf0400056>.
22. Rodríguez, B. A.; Mendoza, S.; Iturriga, M. H.; Castaño-Tostado, E. *J. Food Sci.* **2012**, *77*, C121–C1217. DOI: <https://doi.org/10.1111/j.1750-3841.2011.02487.x>.
23. Ramírez-Jiménez, A. K.; Reynoso-Camacho, R.; Mendoza-Díaz, S.; Loarca-Piña, G. *Food Chem.* **2014**, *161*, 254–260. DOI: <https://doi.org/10.1016/j.foodchem.2014.04.008>.
24. Soto, K.M.; Quezada-Cervantes, C.T.; Hernández-Iturriga, M.; Luna-Bárceñas, G.; Vazquez-Duhalt, R.; Mendoza, S. *LWT - Food Sci. Technol.* **2019**, *103*, 293–300. DOI: <https://doi.org/10.1016/j.lwt.2019.01.023>.
25. Herrera-Rodríguez, S. E.; López-Rivera, R. J.; García-Márquez, E.; Estarrón-Espinosa, M.; Espinosa-Andrews, H. *Food Sci. Biotechnol.* **2019**, *28*, 441–448. DOI: <https://doi.org/10.1007/s10068-018-0499-6>.
26. Skendi, A.; Irakli, M.; Chatzopoulou, P. *J. Appl. Res. Med. Aromat. Plants.* **2017**, *6*, 62–69. DOI: <https://doi.org/10.1016/j.jarmap.2017.02.001>.
27. Bendini, A.; Dell, V.; Antioxiante, A.; Foglie, D. I.; Origano, D. I. *Biol. Nyssana.* **2016**, *7*, 131–139. DOI: <https://doi.org/10.5281/zenodo.200410>.
28. Boroski, M.; Giroux, H.J.; Sabik, H.; Petit, H.V.; Visentainer, J.V.; Matumoto-Pintro, P.T.; Britten, M. *LWT - Food Sci. Technol.* **2012**, *47*, 167–174. DOI: <https://doi.org/10.1016/j.lwt.2011.12.018>.
29. Cortés-Chilata, M. C.; Flores-Martínez, H.; Orozco-Ávila, I.; León-Campos, C.; Suárez-Jacobo, A.; Estarrón-Espinosa, M.; López-Muraira, I. *Molecules* **2021**, *26*, 702. DOI: <https://doi.org/10.3390/molecules26030702>.
30. Heydari, R.; Rashidipour, M. *Int. J. Breast Cancer.* **2015**, *1*. DOI: <https://doi.org/10.1155/2015/846743>.
31. Hamouda, R. A.; Hussein, M. H.; Abo-Elmagd, R. A.; Bawazir, S. S. *Sci. Rep.* **2019**, *9*, 1–17. DOI: <https://doi.org/10.1038/s41598-019-49444-y>.
32. Kumar, M.; Bansal, K.; Gondil, V. S.; Sharma, S.; Jain, D. V. S.; Chhibber, S.; Sharma, R. K.; Wangoo, N. *J. Mol. Liq.* **2018**, *249*, 1145–1150. DOI: <https://doi.org/10.1016/j.molliq.2017.11.143>.
33. Liu, H.; Zhang, H.; Wang, J.; Wei, J. *Arab. J. Chem.* **2017**, *13*, 1011–1019. DOI: <https://doi.org/10.1016/j.arabjc.2017.09.004>.
34. Verma, A.; Mehata, M. S. *J. Radiat. Res. Appl. Sci.* **2016**, *9*, 109–115. DOI: <https://doi.org/10.1016/j.jrras.2015.11.001>.
35. Ashkarran, A.; Bayat, A. *Int. Nano Lett.* **2013**, *3*, 50. DOI: <https://doi.org/10.1186/2228-5326-3-50>.
36. Huang, X.; El-Sayed, M. A. *J. Adv. Res.* **2010**, *1*, 13–28. DOI: <https://doi.org/10.1016/j.jare.2010.02.002>.
37. Marciniak, L.; Nowak, M.; Trojanowska, A.; Tylkowski, B.; Jastrzab, R. *Materials.* **2020**, *13*, 1–12. DOI: <https://doi.org/10.3390/ma13235444>.
38. Rawat, V.; Sharma, A.; Bhatt, V.P.; Singh, R.P.; Maurya, I.K. *Mater. Today Proc.* **2020**, *29*, 911–916. DOI: <https://doi.org/10.1016/j.matpr.2020.05.274>.
39. Khan, M.; Tareq, F.; Hossen, M.A.; Roki, M.N.A.M. *J. Eng. Sci. Technol.* **2018**, *13*, 158–166.
40. Pallela, P.N.V.K.; Ummey, S.; Ruddaraju, L.K.; Pammi, S.V.N.; Yoon, S.G. *Microb. Pathog.* **2018**, *124*, 63–69. DOI: <https://doi.org/10.1016/j.micpath.2018.08.026>.
41. Amaliyah, S.; Sabarudin, A.; Masruri, M.; Sumitro, S.B. *Appl. Pharm. Sci.* **2022**, *12*, 103–114. DOI: <https://doi.org/10.7324/JAPS.2022.120311>.

42. Otunola, G.; Afolayan, A.; Ajayi, E.; Odeyemi, S. *Pharmacogn. Mag.* **2017**, *13*, 201. DOI: https://doi.org/10.4103/pm.pm_430_16.
43. Black, C.; Haughey, S. A.; Chevallier, O. P.; Galvin-King, P.; Elliott, C. T. *Food Chem.* **2016**, *210*, 551–557. DOI: <https://doi.org/10.1016/j.foodchem.2016.05.004>.
44. Barbieri, N.; Sanchez-Contreras, A.; Canto, A.; Cauich-Rodriguez, J. V.; Vargas-Coronado, R.; Calvo-Irabien, L. M. *Ind. Crops Prod.* **2018**, *121*, 114–123. DOI: <https://doi.org/10.1016/j.indcrop.2018.04.081>.
45. Li, R.; Chen, Z.; Ren, N.; Wang, Y.; Wang, Y.; Yu, F. *J. Photochem. Photobiol. B: Biol.* **2019**, *199*, 111593. DOI: <https://doi.org/10.1016/j.jphotobiol.2019.111593>.
46. Zhang, X.; Gao, C.; Lü, S.; Duan, H.; Jing, N.; Dong, D.; Shi, C.; Liu, M. *J. Mater. Chem. B*, **2014**, *2*, 5452–5460. DOI: <https://doi.org/10.1039/c4tb00905c>.
47. Nersisyan, H. H.; Lee, Y. J.; Joo, S. H.; Han, S. K.; Lee, T. H.; Lee, J. S.; An, Y. S.; Lee, J. H. *Cryst. Eng. Comm.* **2015**, *17*, 7535–7542. DOI: <https://doi.org/10.1039/c5ce01367d>.
48. Carbone, K.; Paliotta, M.; Micheli, L.; Mazzuca, C.; Cacciotti, I.; Nocente, F.; Ciampa, A.; Dell'Abate, M. T. *Arab. J. Chem.* **2019**, *12*, 597–609. DOI: <https://doi.org/10.1016/j.arabjc.2018.08.001>.
49. Vimbela, G. V.; Ngo, S. M.; Frazee, C.; Yang, L.; Stout, D. A. *Int. J. Nanomed.* **2017**, *12*, 3941–3965. DOI: <https://doi.org/10.2147/IJN.S134526>.
50. Ruíz-Baltazar, Á. D. J.; Reyes-lópez, S. Y.; Larrañaga, D.; Estévez, M.; Pérez, R. *Results Phys.* **2017**, *7*, 2639–2643. DOI: <https://doi.org/10.1016/j.rinp.2017.07.044>.
51. Abbaszadegan, A.; Ghahramani, Y.; Gholami, A.; Hemmateenejad, B.; Dorostkar, S.; Nabavizadeh, M.; Sharghi, H. *J. Nanomater.* **2015**, *1*. DOI: <https://doi.org/10.1155/2015/720654>.
52. Arana-Sánchez, A.; Estarrón-Espinosa, M.; Obledo-Vázquez, E. N.; Padilla-Camberos, E.; Silva-Vázquez, R.; Lugo-Cervantes, E. *Lett. Appl. Microbiol.* **2010**, *50*, 585–590. DOI: <https://doi.org/10.1111/j.1472-765X.2010.02837.x>.
53. Rueda, E.; Juvera, J.; Romo, I.; Holguín, R. *Rev. Mexicana Cienc. Agri.* **2018**, *20*, 4251–4261.